



# Starch/Poly(butylene succinate) Compatibilizers: Effect of Different Reaction-Approaches on the Properties of Thermoplastic Starch-Based Compostable Films

Barbara Fahrngruber<sup>1</sup> · Marta Fortea-Verdejo<sup>2</sup> · Rupert Wimmer<sup>3</sup> · Norbert Mundigler<sup>4</sup>

Published online: 11 November 2019

© Springer Science+Business Media, LLC, part of Springer Nature 2019

## Abstract

The property profile of thin thermoplastic starch (TPS)/poly(butylene succinate) (PBS) films was investigated and the potential improvement, which can be achieved due to the utilization of hydrophilic/hydrophobic compatibilizer systems, was assessed. The evaluation in terms of morphology exhibited a very good TPS dispersion (under optimized processing conditions) within the polyester matrix, while an average particle size of 1.5  $\mu\text{m}$  was obtained. Two different raw material approaches were applied for the preparation of the compatibilizers: (a) native corn starch and (b) destructured TPS. In the course of the compounding process 0.5 and 1.0 wt% of the two compatibilizer systems (a) and (b) were added. In comparison, the addition of the TPS-based compatibilizer resulted in improved incorporation of TPS within the polyester matrix, which was accompanied by higher tensile strength and tear resistance. Explanations for this observation could be that pre-plasticized starch provides a larger reaction surface and enables better homogenization during the course of compounding. In contrast, for native starch the reaction only can take place at the granule surface and thus, the compatibilization was less efficient. The outcome of this investigation is a compostable film material with high bio-based content, which exhibits great potential for single-use, light-weight packaging applications.

**Keywords** Thermoplastic starch · Reactive extrusion · Compatibilization · Compostability · Biomaterials characterization

**Electronic supplementary material** The online version of this article (<https://doi.org/10.1007/s10924-019-01601-0>) contains supplementary material, which is available to authorized users.

✉ Barbara Fahrngruber  
barbara.fahrngruber@agrana.com

<sup>1</sup> Agrana Research & Innovation Center GmbH, Josef-Reither-Straße 21-23, 3430 Tulln, Austria

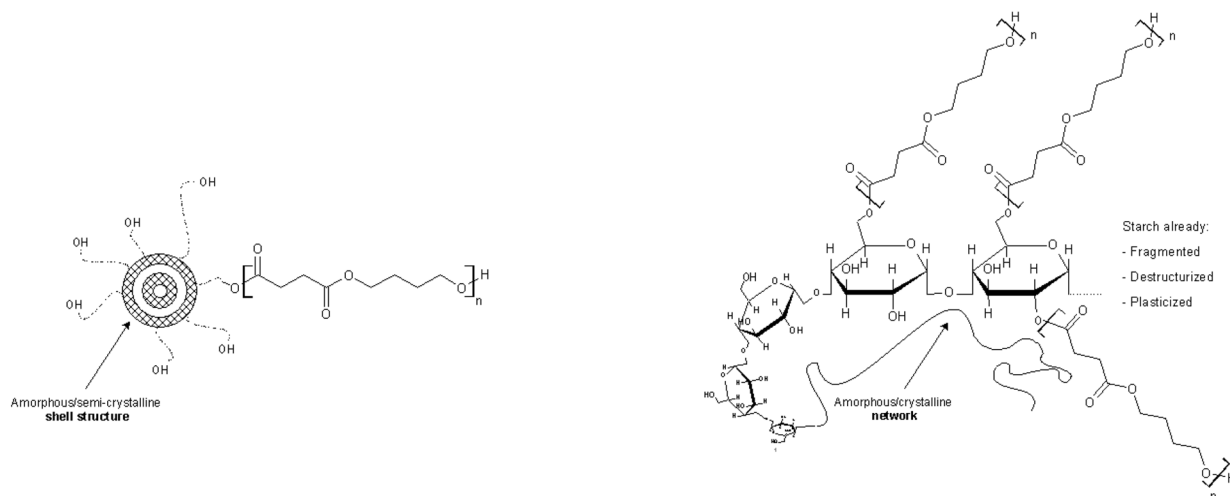
<sup>2</sup> Polymer and Composite Engineering (PaCE) Group, Institute of Materials Chemistry and Research, Faculty of Chemistry, University of Vienna, Währingerstraße 42, 1090 Vienna, Austria

<sup>3</sup> Institute for Wood Technology and Renewable Materials, University for Natural Resources and Life Sciences, Vienna, Konrad Lorenz Strasse 24, 3430 Tulln, Austria

<sup>4</sup> Institute for Natural Materials Technology, University for Natural Resources and Life Sciences, Vienna, IFA Tulln, Konrad Lorenz Strasse 20, 3430 Tulln, Austria

## Introduction

During the past two decades thermoplastic starch (TPS)-based polyester compounds have been extensively investigated since starch is used in polymer formulations for three major purposes: (1) cost-reduction, (2) increase in biodegradation speed, and (3) increase in bio-based content [1]. Different strategies for the compatibilization of TPS-polyester mixtures have been developed and characterized such as carboxylic acid- [2, 3], maleic anhydride- [4–7] and glycidyl methacrylate-based systems [8], as well as binary/ternary blend formulations [9–11]. Many approaches have focused on the optimization of compound formulations consisting of starch and petroleum-based polybutylene adipate-co-terephthalate (PBAT), because the polyester exhibits a market competitive price and is readily available. Polyesters, which are (completely or only partially) obtained from natural building blocks, have attracted attention in recent years because of their renewable, bio-based character. Among them, poly(butylene succinate) (PBS), which is a biodegradable polyester (already

**(a) Native starch-based compatibilizer****(b) Thermoplastic starch (TPS)-based compatibilizer**

**Fig. 1** Compatibilizer systems (proposed reaction mechanism) based on **a** native, granular starch and **b** thermoplastic starch in combination with poly (butylene succinate)

commercially available) with a bio-based carbon content between 35 and 50% (which will further increase in the near future), is of great interest [12–14]. Therefore, PBS exhibits potential as a compound-partner in combination with TPS, intended for the preparation of cost-effective and sustainable film materials. As in the case of TPS/PBAT mixtures, the production of high-quality compounds consisting of TPS and PBS is difficult, because the miscibility of the two polymers is restricted due to differences in viscosity and interfacial tension [15–17].

In this study, two approaches are addressed with respect to the compatibilization of TPS/PBS compounds during reactive extrusion: the preparation of a compatibilizer system based on (1) native starch, and (2) pre-plasticized/destructurized starch, i.e. TPS (Fig. 1).

To generate a better understanding for TPS/PBS mixtures as potential future compounding partners, three hypotheses are stated: (1) The two mentioned reactive compatibilizer approaches enable different interactions with starch (in TPS) and polyester. In case of the native starch-based compatibilizer the reaction can only take place at the granule surface, which restricts the compatibilization-efficiency as well as the production of thin film materials with high surface quality (as the starch granules to some extent are likely to act as defects inside of the compound matrix). The already plasticized TPS-based system is expected to enable a better homogenization during compounding, providing a larger interaction surface since the reaction between starch and PBS can occur throughout the compatibilizer-system. (2)

The addition of the TPS-based compatibilizer improves the incorporation of TPS within the PBS matrix. (3) The mechanical properties of film materials consisting of TPS and PBS are influenced by the compatibilizer concentration. Particularly, the mechanical strength is expected to improve when the compatibilizer is added. Finally, the disintegration of the produced TPS/PBS films under home composting conditions is reported.

The overall goal of this research is the development of a flexible plastic material, which is suitable to replace single-use, petro-based and persistent packaging. To meet the market-requirements, the production of thin film materials (layer thicknesses of 50  $\mu\text{m}$  and lower) must be possible, whereby a preferably high elongation as well as a mechanical strength of at least 30 MPa, and tear resistance of 50 N/mm, are considered as state of the art [2, 18, 19]. The utilization of TPS in plastic-packaging usually introduces hydrophilic characteristics due to the hydrophilic functionalities that are present in starch [19]. The influence of compatibilization on the water vapor barrier is addressed in the present investigation. A full degradation under composting conditions is targeted, since a controlled, separate waste collection cannot be granted in the case of light-weight, single-use packaging.

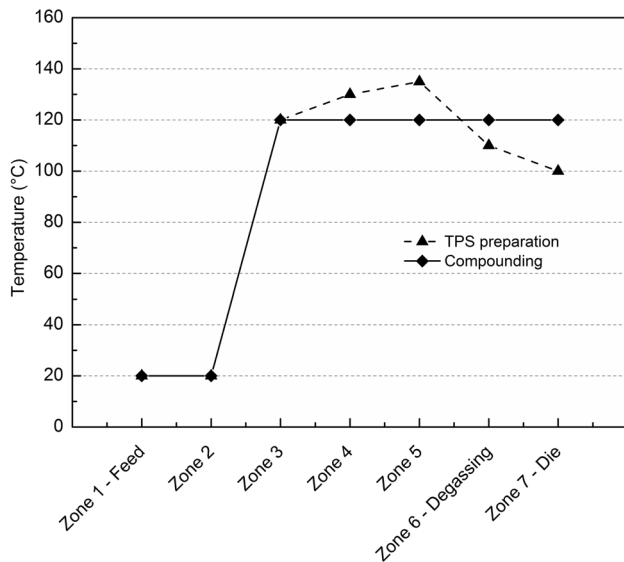


**Fig. 2** Temperature (°C) profile applied during extrusion, for the preparation of thermoplastic starch as well as for compounding

## Experimental Part

### Materials and Methods

#### TPS Extrusion

To obtain TPS, native corn starch (Agrana Stärke, Austria) was deconstructed within a co-rotating twin screw extruder (27D, Theysohn, Switzerland) at a screw speed of 200 rpm. Glycerol (13 wt%, Brenntag, Austria), and stearic acid (2.0 wt%, Sigma Aldrich) were added as plasticizer and processing aid (applied temperature profile see Fig. 2).

#### Compatibilizer Preparation

The starch-based as well as the TPS-based compatibilizer were prepared in accordance with the methodology described by Suchao-in, Koombhongse & Chirachanchai [16], whereat reaction time, batch size and reactant ratio were slightly adapted. Twenty grams of PBS (film type, MCPP Germany GmbH) were dissolved in chloroform (Honeywell™, Germany) in a three-neck round-bottom 1000 ml flask. As soon as PBS had fully dissolved the starch (100 g, pre-dried) [or in case of the TPS-based compatibilizer the ground TPS powder (120 g)] was added to the solution. Afterwards, the mixture was stirred for 2 h, before the flask was flushed with nitrogen and N,N'-dicyclohexylcarbodiimide (DCC, 30 g) (Sigma Aldrich, Germany) was added. After 48 h of reaction time under constant stirring at room temperature the obtained

**Table 1** Experimental setup

Concentration (wt%)	Starch-based compatibilizer	TPS-based compatibilizer
0	Control	
0.5	05St	05TPS
1.0	10St	10TPS

suspension was centrifuged to remove residual, unreacted starch/TPS. The supernatant was further treated with acetone (Sigma Aldrich, Germany) to precipitate the reaction product, which was then purified by repeated washing with ethanol (Sigma Aldrich, Germany). The reaction product was dried at 40 °C for 48 h. The compatibilizer preparation was also conducted without DCC (control), in order to show the absence of an interaction between starch and PBS without the reagent. The stability of the suspended reaction products in chloroform (10 mg compatibilizer suspended in 2 ml chloroform) was taken as a qualitative measure for the compatibilizer efficiency [5].

#### Compounding

Compounding of TPS with PBS (1:1) was conducted via extrusion using a co-rotating twin screw extruder (27D, Theysohn, Switzerland). Initially, four different screw speeds (100, 200, 300 and 400 rpm) were applied to evaluate the optimum processing range. The incorporation of TPS within the polyester matrix was investigated by means of iodine testing. For this purpose, the prepared compound granules were exposed to iodine/potassium-iodine solution (Lugol's solution diluted 1 wt%, Sigma Aldrich, Germany) and the evolving color effects were used to differentiate between a sufficient and a non-sufficient incorporation of TPS inside the polyester matrix (solution colored → non-sufficient incorporation; only granules colored/solution yellow → incorporation and fine distribution). The addition of the two compatibilizer systems at concentrations of 0.5 and 1.0 wt% (with respect to the TPS share) was conducted via a micro-dosing unit (Brabender, Germany) at optimum screw speed only (Table 1).

#### Flat Film Preparation

Flat films were prepared using a small-scale flat film extrusion line (Optical Control Systems, Germany) at 160 °C, 20 rpm, and a haul off speed of 3.5 m/min. A film thickness between 40 and 50 μm was obtained (average

thickness measured over 10 points, thickness testing instrument Kaefer, Germany).

## Characterization

### Scanning Electron Microscopy (SEM)

The compounds were fractured in liquid nitrogen and treated with hydrochloric acid to remove the dispersed starch particles. Prior to microscopic analysis the samples were gold-coated using a sputter coater (JEOL®, JCM-1200 Fine Coater). The particle surface was then investigated via an electron microscope (JEOL®, JCM 5000 NeoScope, 10 kV, high-vacuum mode, China), which was equipped with a secondary electron detector. The film surfaces were investigated by means of a microscope camera (DigiMicro, dnt, Germany).

### Fourier Transform Infrared Spectroscopy (FTIR)

Infrared spectra were recorded using a FTIR spectrometer (Bruker®, Alpha Sample Compartment RT-DLaTGS, Austria) in attenuated total reflectance (ATR) mode, at a spectral resolution of  $2\text{ cm}^{-1}$  (wavenumber range  $400\text{--}4000\text{ cm}^{-1}$ ). The shown FTIR spectra are an average of three independent measurements each, with vector normalization and baseline correction (rubberband method), computed via OPUS software, version 7.5.

### Differential Scanning Calorimetry (DSC)

The evaluation of the thermal compound characteristics happened via differential scanning calorimetry, using a DSC 214 Polyma (Netzsch, Germany). Measurements were conducted under a constant nitrogen flow of 50 ml/min. The temperature cycle involved a heating up to  $160\text{ }^{\circ}\text{C}$ , with a subsequent cooling to  $-50\text{ }^{\circ}\text{C}$ . The measurements were done in triplicate. The determination of relaxation processes in TPS associated with the glass transition were monitored via the glass transition temperature ( $T_g$ , point of inflection). For the determination of the required transition energy different heating rates (10, 20, 30 and  $40\text{ K/min}$ ) were applied. A linear relationship was constituted with  $\ln \beta$  (heating rate) and the reciprocal glass transition temperature ( $1/T_g$ ). The calculation of the activation energy  $E_a$  was conducted from the slope of the obtained  $\ln \beta$  versus ( $1/T_g$ ) graphs (Eq. 1,  $R$  represents the gas constant) [20–23]:

$$\ln \beta = -\frac{E_a}{R} \cdot \frac{1}{T_g} + \text{constant} \quad (1)$$

The change in heat capacity  $\Delta c_p$  was taken as an indicator for the molecular arrangement present in TPS, which directly relates to the presence of disordered, amorphous structures [24, 25].

### Size Exclusion Chromatography (SEC)

To identify possible influences due to molecular weight related changes, the weight average molecular weight ( $M_w$ ) was determined with a Thermo Fisher Scientific chromatograph (Dionex Ultimate 3000, Austria). For the characterization of the polyester-phase the chromatograph was equipped with a styrene–divinylbenzene copolymer column system ( $1000\text{--}1,000,000\text{ \AA}$ , chloroform,  $0.6\text{ ml/min}$ ), and a refractive index detector (Refractomax 520), with poly(methyl methacrylate) standards used for calibration purposes. The determination of the TPS-phase was conducted with a polyhydroxymethacrylate copolymer column system ( $100\text{--}30,000\text{ \AA}$ , sodium nitrate,  $0.7\text{ ml/min}$ ). For sample detection a refractive index detector (RI-101) was used. Monodisperse pullulan standards were applied for calibration purposes. Measurements were conducted in triplicate.

### Mechanical Material Properties





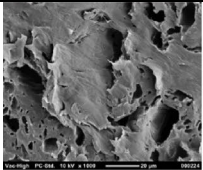
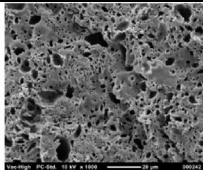
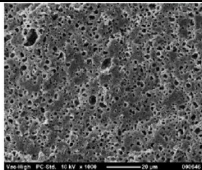
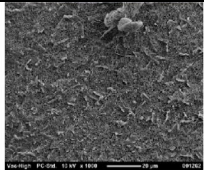
The determination of the mechanical film properties was conducted on a Zwick Roell (Germany) universal testing machine. Measurement and sample geometry followed ÖNORM EN ISO 527-3 standard, with a clamp distance of 105 mm. A cross-head speed of  $100\text{ mm/min}$  was applied for the measurement of stress and elongation (measured via mechanical extensometer). For each film sample at least five specimens were tested (in machine direction = longitudinal production direction).

Tear resistance was determined according to ÖNORM ISO 34-1:2005. Tests were carried out using an angle test sample (Graves) with notch (method B). For each experiment five samples were tested, using a test speed of  $100\text{ mm/min}$ . Preload was set to  $0.2\text{ N}$ , and a  $2\text{ kN}$  load cell was used. The clamp distance equaled 60 mm.

### Water Vapor Barrier

The water vapor transmission rate (WVTR) was obtained using a water vapor transmission tester (W3/031, Labthink, China). The tests were performed at  $38\text{ }^{\circ}\text{C}$  and 90% RH following ASTM E96. The tested area was circular shaped with a diameter of 74 mm. Prior to the test, a 1 h preheating step was performed. 10 weighting cycles were performed per sample in 30 min intervals.

**Table 2** Process optimization for the sufficient incorporation of TPS within the polyester matrix

Screw speed	100 rpm	200 rpm	300 rpm	400 rpm
Iodine test				
Microscopy				
Average particle size (μm)	$52.0 \pm 5.7^a$	$24.3 \pm 2.8^b$	$7.2 \pm 1.1^c$	$1.5 \pm 0.3^d$

Numbers followed by the same letter are not significantly different (significant difference at  $p < 0.05$ )

### Disintegration Testing

The flat films were weighed, cut to a size of  $10 \times 15$  cm and placed on a mesh, which was then fixed within a wooden frame by using staples [26]. The samples were buried in a mixture consisting of soil and fresh compost (1:1). The temperature was kept constant at  $25^\circ\text{C}$  (drying closet type Memmert, Germany). After 10, 20 and 30 days the samples were removed and evaluated with respect to their optical appearance (photo documentation). At the end of the test, the remaining particles with a particle size bigger than 2 mm were determined gravimetrically. Samples and the utilized soil/compost mixtures were sieved through a 2 mm mesh. Remaining soil particles were removed and the film-fragments were conditioned in a drying chamber prior to weighing.

### Statistical Evaluation

Analysis of variance (ANOVA) was conducted, followed by Tukey multiple comparison post-hoc test. Mean differences were tested for statistical significance ( $p < 0.05$ , Minitab 17.0).

## Results and Discussion

### Compounding

#### Optimizing the Process (Without Compatibilizer)

The TPS incorporation within the polyester matrix, the morphological appearance, and particle sizes of the

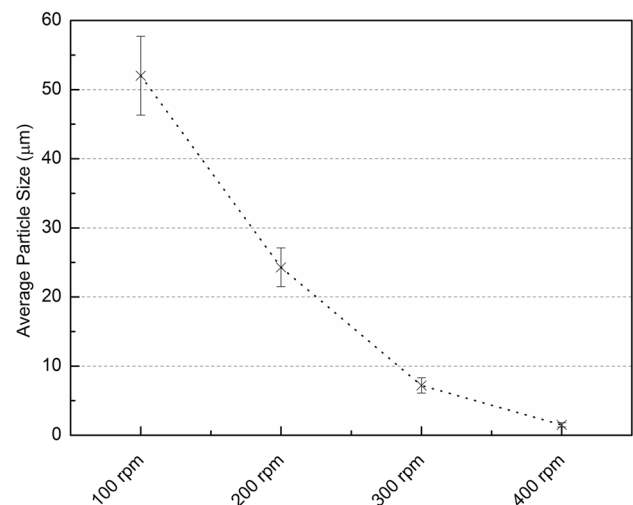


**Fig. 3** Average particle size of the dispersed TPS as a function of extrusion screw speed

compounded granules were evaluated via extrusion trials at 100, 200, 300 and 400 rpm (Table 2).

It is visible that the incorporation of TPS inside of the polyester matrix has improved, at higher screw speeds. At 100 and 200 rpm the compound granules retained a light color and the iodine solution was dark blue colored. The dark blue color is evidence for a complete separation of starch from the polyester matrix (into the test solution), which indicates an insufficient TPS inclusion. At 400 rpm the obtained particle sizes were small, with the compounds remaining stable when in contact with the test solution (Fig. 3).

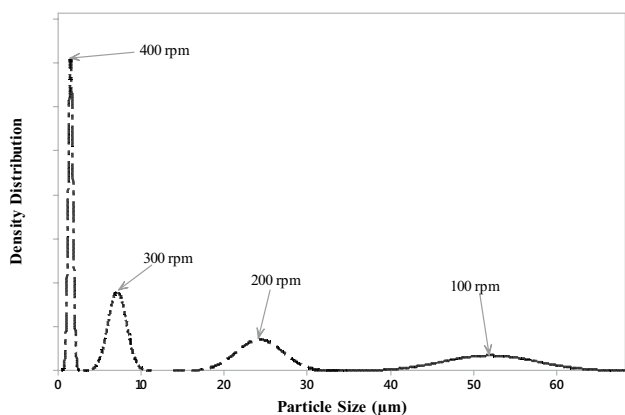


**Fig. 4** Particle size distribution of the dispersed TPS along with increasing extrusion screw speed (100 rpm → 400 rpm)

It was also observed that a more uniform particle size distribution was achieved at elevated screw speeds (Fig. 4).

Film materials produced with compounds prepared at low screw speed (100 and 200 rpm) exhibited instable processability, with process interruptions due to reduced melt strength, along with a noticeable film surface roughness (Fig. 5). In case of the compound materials produced at 300 rpm as well as 400 rpm the surface quality overall improved, with the quality being still better at 400 rpm than at 300 rpm. Consequently, 400 rpm was taken as the standard processing parameter for the preparation of the TPS/PBS compounds in the present study.

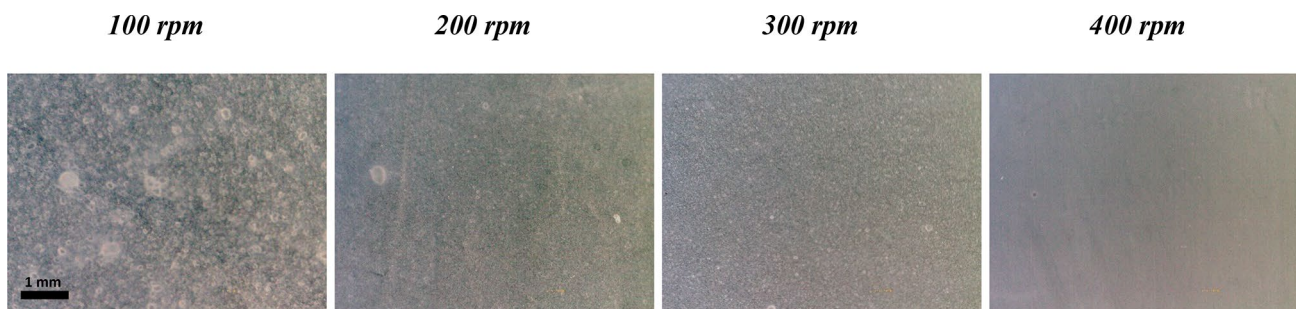


**Fig. 5** Surface roughness of the film materials made from TPS/PBS compounds, which were produced at varying screw speeds

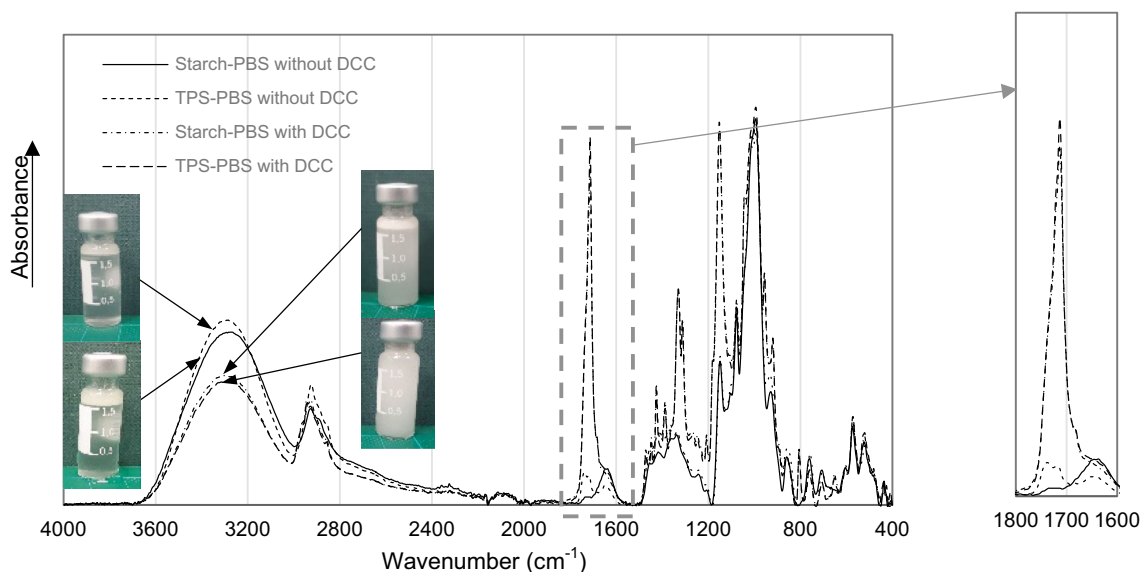


**Fig. 6** FTIR spectra of the produced compatibilizers with and without reagent (DCC) addition (on the basis of native starch and TPS); stability of the obtained compatibilizers in chloroform

## Incorporation of Compatibilizers During Compounding

**Structural Compatibilizer Characterization** Figure 6 shows FTIR spectra of the prepared native starch- and TPS-based (i.e. starch-PBS, TPS-PBS) compatibilizer systems. Additionally, the preparation of the compatibilizers was conducted without the reagent DCC (starch without DCC: only adsorbed water visible at  $1650\text{ cm}^{-1}$ , TPS without DCC: adsorbed water + stearic acid visible at  $1650\text{ cm}^{-1}$  and  $1720\text{ cm}^{-1}$ , respectively). The recorded spectra demonstrate that it's not possible to achieve a chemical link between starch and PBS without DCC. Without DCC, the PBS is removed due to precipitation and the applied washing steps conducted during product purification. In case of the esterification with DCC a clearly defined carbonyl peak ( $1710\text{ cm}^{-1}$ ) is visible, which is representative for an interaction between starch/TPS and PBS [27, 28].

Further, the formation of hydrogen bonds (peak intensity changes at  $3300\text{ cm}^{-1}$ ) was reduced for the esterified systems starch-PBS and for TPS-PBS.

The solubility in chloroform was influenced due to the functionalization with DCC and PBS [5]. The control samples (without DCC) precipitated immediately, while the DCC modified samples enabled a formation of a suspension with variable stability (TPS-PBS → stable, Starch-PBS → incomplete precipitation). Overall, the formation of compatibilizers with reduced hydrophilicity was verified (TPS-PBS completely, Starch-PBS partially). A method for the quantitative evaluation of the grafting efficiency is currently under development.

## Compound Morphology

Table 3 shows the fractured compound surfaces after removal of the TPS phase via hydrochloric acid. The microscopic images confirm the uniform and fine distribution of TPS inside of the polyester matrix across all samples. Thus, side effects due to significant variations in particle size can be excluded.

## Compound Characterization

### Differential Scanning Calorimetry

Glass transition temperatures for the TPS phase within the compounded materials, and activation energies are shown in Table 4 (Figure S1).

Comparatively, a shift in  $T_g$  (endothermic hump around  $70\text{ }^\circ\text{C}$ ) with increasing heating rate towards higher temperatures can be deduced from a demobilization of molecules due to stress [29]. Figure 7 demonstrates the investigated activation energy plots.

Apparently, slope changes and thus changes in activation energy were achieved through the addition of the compatibilizer (activation energy increased for samples 10St, 05TPS and 10TPS). This effect can be deduced from a reduced molecule mobility (starch immobilization because of increased interaction with the polyester matrix) which was caused due to an enhanced molecular entanglement, and is accompanied by changes in free volume [30]. Furthermore, it is likely that glycerol-esters (as a compatibilizer side-product in the case of 05TPS and 10TPS) were able to form interactions between starch and the polyester, and thus acted like small anchor points, which further enhanced the interaction between the two phases [31].

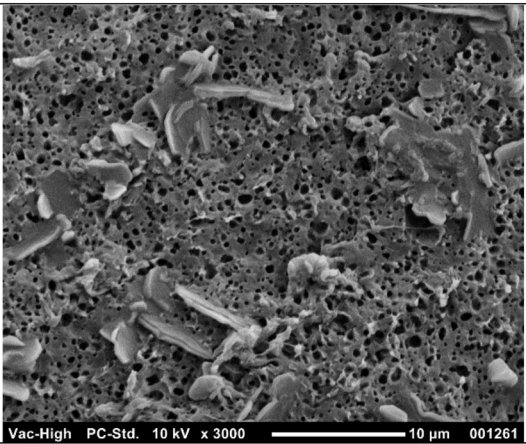
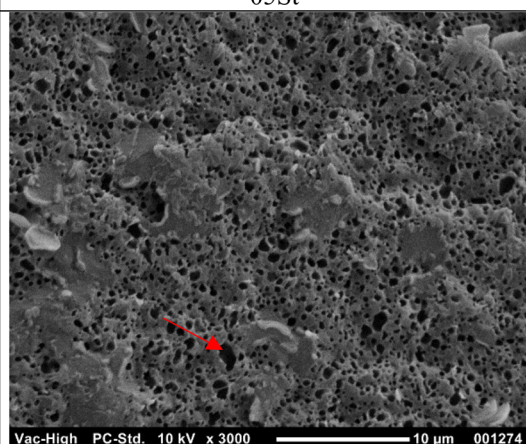
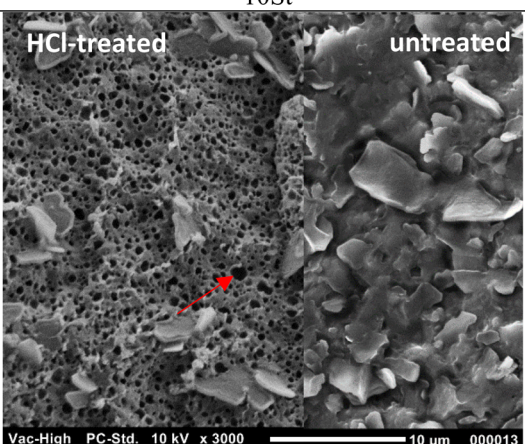
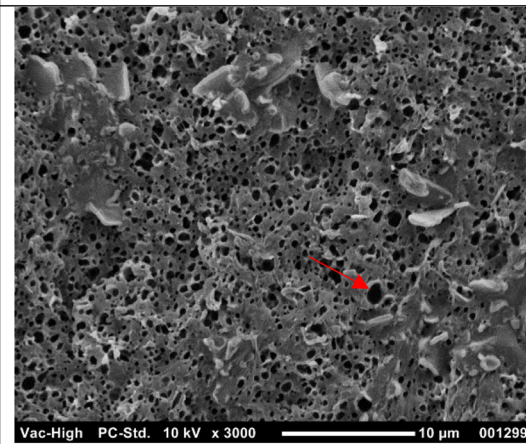
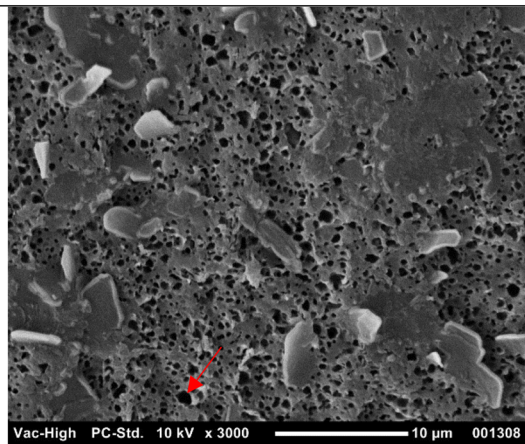
Table 5 shows the heat capacity changes, which were observed for the investigated compound materials.  $\Delta c_p$  was used as indicator for the structural arrangement within TPS. The heat capacity step can be directly correlated with the presence of disordered (amorphous) regions. The observed increase in  $\Delta c_p$  (control → 10TPS) leads to the conclusion that the compatibilizer addition promoted the growth of amorphous TPS-structures. The effect was more pronounced (statistically significant) at low heating rates (10 and 20 K/min) [32–36].

### Size Exclusion Chromatography

The average molecular weights for TPS and polyester phases are listed in Table 6 (Figure S2).

Since the polyester constitutes the continuous phase in the investigated TPS/PBS systems (verified via scanning electron microscopy), the polyester has to fulfil essential functions such as the transmittance and distribution of stress to the dispersed particles as well as the suppression of cracks formed as a response to mechanical stress. According to the obtained results the polyester phases weight average molecular weight did not change with added compatibilizers. Thus, effects that could potentially evolve due to a matrix weakening because of molecular weight changes can be excluded [37]. In contrast, the starch phases have shown molecular weight changes (significant at the highest compatibilizer concentrations 10St as well as 10TPS). These findings correlate with torque data, as observed during the compounding experiments. According to literature there are two main mechanisms that could be responsible for the described observations: (1) the addition of the compatibilizer led to a reduced interaction between TPS and water (the used TPS contains water that potentially acts as a plasticizer), which has further provoked a slight increase in viscosity; [38] (2) the formation of clusters, which exhibited a higher susceptibility to shear-induced degradation [39, 40].

**Table 3** Morphology of the fractured and etched compounds to demonstrate the distribution of TPS inside of the polyester matrix

Control	
	
<small>Vac-High PC-Std. 10 kV x 3000 10 μm 001261</small> $1.5 \pm 0.3^a$	
05St	10St
	
<small>Vac-High PC-Std. 10 kV x 3000 10 μm 001274</small> $1.4 \mu\text{m} \pm 0.2^a$	<small>Vac-High PC-Std. 10 kV x 3000 10 μm 000013</small> $1.1 \mu\text{m} \pm 0.3^a$
05TPS	10TPS
	
<small>Vac-High PC-Std. 10 kV x 3000 10 μm 001299</small> $1.4 \mu\text{m} \pm 0.3^a$	<small>Vac-High PC-Std. 10 kV x 3000 10 μm 001308</small> $1.3 \mu\text{m} \pm 0.2^a$

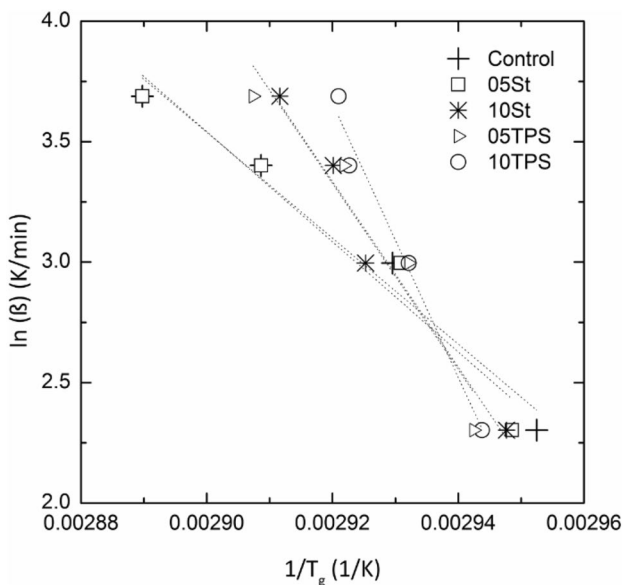
Numbers followed by the same letter are not significantly different (significant difference at  $p < 0.05$ ); See Table 1 for sample identification



**Table 4** Glass transition temperatures at varying heating rates (10, 20, 30 and 40 K/min), calculated activation energies ( $E_a$ ),  $R^2$ =coefficient of determination

	T <sub>g</sub> °C (10 K/min)	T <sub>g</sub> °C (20 K/min)	T <sub>g</sub> °C (30 K/min)	T <sub>g</sub> °C (40 K/min)	E <sub>a</sub> (kJ/mol)	R <sup>2</sup>
Control	65.6 ± 0.6	68.2 ± 0.0	70.7 ± 0.8	72.9 ± 1.0	188.2 ± 22.9 <sup>a</sup>	0.96
05St	66.0 ± 0.4	68.1 ± 0.8	70.7 ± 0.8	72.9 ± 0.4	188.1 ± 10.1 <sup>a</sup>	0.93
10St	66.1 ± 0.4	68.7 ± 0.1	69.3 ± 1.4	70.3 ± 1.4	325.5 ± 32.0 <sup>b</sup>	0.92
05TPS	66.7 ± 0.4	67.9 ± 0.6	69.1 ± 1.8	70.8 ± 0.0	303.0 ± 17.9 <sup>b</sup>	0.96
10TPS	66.6 ± 0.1	67.9 ± 1.1	69.0 ± 0.0	69.2 ± 1.0	406.2 ± 29.2 <sup>c</sup>	0.97

Numbers followed by the same letter are not significantly different (significant difference at  $p < 0.05$ ); See Table 1 for sample identification

**Fig. 7** Heating rate dependency of glass transition temperature for the starch phase within TPS/PBS compound materials

## Film Characterization

### Mechanical Film Characteristics

Results (Figs. 8 and S3) show a significant increase in tensile strength and tear resistance for the TPS-based compatibilizer at both concentrations 0.5 and 1.0 wt%. In case of the starch-based compatibilizer a significant increase of tensile strength and tear resistance was only visible at 1.0 wt%. The

**Table 5** Changes in heat capacity for the investigated compound materials under varying heating rates (10, 20, 30 and 40 K/min)

	$\Delta c_{p10}$ (J/g K)	$\Delta c_{p20}$ (J/g K)	$\Delta c_{p30}$ (J/g K)	$\Delta c_{p40}$ (J/g K)
Control	0.172 ± 0.001 <sup>a</sup>	0.151 ± 0.002 <sup>a</sup>	0.143 ± 0.037 <sup>a</sup>	0.125 ± 0.006 <sup>a</sup>
05St	0.205 ± 0.013 <sup>a,b</sup>	0.173 ± 0.005 <sup>a,b</sup>	0.136 ± 0.025 <sup>a</sup>	0.118 ± 0.008 <sup>a</sup>
10St	0.209 ± 0.003 <sup>a,b</sup>	0.171 ± 0.017 <sup>a,b</sup>	0.146 ± 0.015 <sup>a</sup>	0.140 ± 0.022 <sup>a</sup>
05TPS	0.211 ± 0.001 <sup>a,b</sup>	0.186 ± 0.001 <sup>b</sup>	0.136 ± 0.015 <sup>a</sup>	0.111 ± 0.011 <sup>a</sup>
10TPS	0.228 ± 0.004 <sup>b</sup>	0.187 ± 0.007 <sup>b</sup>	0.148 ± 0.013 <sup>a</sup>	0.153 ± 0.043 <sup>a</sup>

Numbers followed by the same letter are not significantly different (significant difference at  $p < 0.05$ ); See Table 1 for sample identification

TPS dispersion has proven to be comparable for the investigated formulations and thus, cannot be the reason for the observed changes in mechanical performance (on  $\mu\text{m}$  scale). The observed reduction in TPS-average molecular weight has probably led to changes in viscosity, which induced an enhanced miscibility of a defined particle fraction at sub-micrometer scale (not visible on the obtained SEM micrographs). This subject needs to be further addressed. Besides that, it has been observed before that the utilization of hydrophilic/hydrophobic compatibilizers in 2-phase systems provokes an improvement in interfacial adhesion, which furthermore leads to higher tensile strength. Here, literature is referring to two mechanisms: (1) changes in the maximum bearable load due to changes in adhesion between matrix and dispersed particle [41] and (2) a restriction in molecule mobility due to the formation of a structural network [42]. In this investigation, the PBS-side chains, which are present in the compatibilizer-systems, are expected to enhance the molecular entanglement within the compound system.

### Water Vapor Barrier

Water vapor permeability (WVP) and water vapor transmission rates (WVTR) are listed in Table 7.

No significant changes were found for mass gain and WVTR. Apparently, the WVP only slightly increased in the case of 10TPS. In principle, the utilization of TPS in polyester formulations is reported to increase the WVP characteristics [43]. Within the compound-material even small alterations in film thickness could have led to the observed deviations in WVP. As reported in the literature, the

thickness influences the structural arrangement, which could furthermore affect the mass transfer across the film [44]. Another explanation could be the improved incorporation of TPS within the polyester matrix, due to which the hydrophilic characteristics of the starch component became more dominant. Furthermore, it is likely that the compatibilization

and the related interaction with the polyester has affected the formation of a close intermolecular arrangement in TPS, which additionally facilitated the WVP. Literature confirms that the introduction of hydrophobic components in compound formulations does not necessarily result in a reduced WVP. The WVP depends on versatile factors such as the formation of pores and channels, which furthermore affect the flow profile within the materials structure and thus, the permeability characteristics [45].

**Table 6** Weight average molecular weights for the two compound constituents: (1) thermoplastic starch, (2) polyester PBS and extrusion-torque (recorded in the course of the compounding process)

	TPS (kDa) $M_w$	PBS (kDa) $M_w$	Torque (%)
Control	123.00 ± 2.12 <sup>a</sup>	161.60 ± 22.00 <sup>a</sup>	53.08 ± 0.07
05St	119.00 ± 0.71 <sup>a</sup>	159.90 ± 13.85 <sup>a</sup>	53.24 ± 0.70
10St	96.05 ± 1.20 <sup>b</sup>	178.50 ± 24.04 <sup>a</sup>	54.79 ± 0.57
05TPS	116.00 ± 0.71 <sup>a</sup>	171.55 ± 23.12 <sup>a</sup>	53.23 ± 0.33
10TPS	69.60 ± 0.42 <sup>c</sup>	177.40 ± 12.86 <sup>a</sup>	56.85 ± 0.24

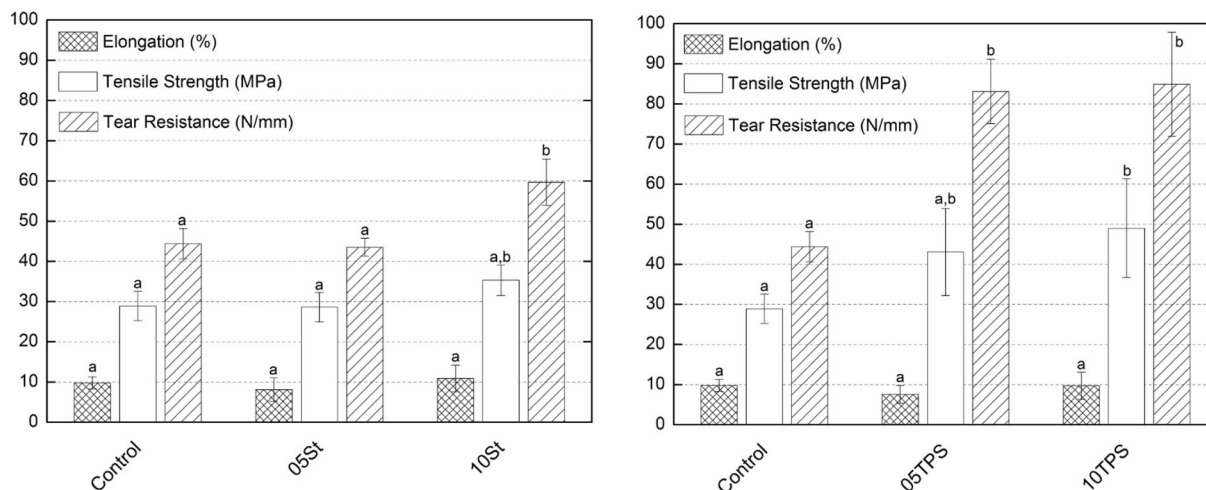
Numbers followed by the same letter are not significantly different (significant difference at  $p < 0.05$ ); See Table 1 for sample identification

## Disintegration

Table 8 shows the optical appearance of the various film types as a function of the disintegration-time.

The images demonstrate the disintegration of the film materials under home composting conditions. After 10 days visible cracks appeared on the surfaces of all samples, which subsequently continued with a transformation into holes (after 20 days of composting). Figure 9 shows the quantitative evaluation of the film material disintegration via (gravimetric) sieving.

## Mechanical film characteristics











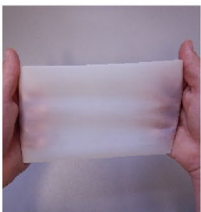











**Fig. 8** Tensile properties of the investigated film materials, for the native starch-based compatibilizer (left), and the TPS-based compatibilizer (right)

**Table 7** Effect of compatibilizers on water vapor transmission rate (WVTR) and water vapor permeability (WVP) of TPS/PBS films

Sample	WVTR (g/m <sup>2</sup> 24 h)	WVP [g cm/(cm <sup>2</sup> s Pa)]	Film thickness (μm)	Mass gain just after test (wt%)
Control	451.9 ± 8.6 <sup>a</sup>	6.6E-13 ± 2.7E-14 <sup>a</sup>	50	6.0 ± 0.7 <sup>a</sup>
05St	443.5 ± 8.2 <sup>a</sup>	6.8E-13 ± 2.0E-14 <sup>a,b</sup>	50	5.9 ± 1.5 <sup>a</sup>
10St	445.3 ± 5.0 <sup>a</sup>	6.9E-13 ± 3.7E-14 <sup>a,b</sup>	45	3.9 ± 1.3 <sup>a</sup>
05TPS	456.7 ± 7.3 <sup>a</sup>	7.0E-13 ± 3.2E-14 <sup>a,b</sup>	45	5.3 ± 0.2 <sup>a</sup>
10TPS	463.7 ± 10.8 <sup>a</sup>	7.5E-13 ± 5.6E-14 <sup>b</sup>	40	5.5 ± 0.5 <sup>a</sup>

Numbers followed by the same letter are not significantly different (significant difference at  $p < 0.05$ ); See Table 1 for sample identification

**Table 8** Disintegration of the investigated film materials after composting for 10, 20 and 30 days

	Initial	10 days	20 days	30 days	Fraction < 2 mm (%)
Control					79.2
05St					77.6
10St					65.5
05TPS					69.2
10TPS					77.7

Due to the beginning destruction and the associated increase in attack surface the microbial activity and hence, the disintegration started to accelerate after 20 days composting time. Figure 10 shows the formation of cracks and microbial attack, as processes appearing during composting.

The disintegration of the control sample proceeded slightly faster. To verify the significance of this observation further investigations are required.



**Fig. 9** Quantitative evaluation of the film-disintegration

## Conclusions

The production of thin film materials based on bioplastics requires a defined polymer compound quality. Huge starch particles affect the melt strength and thus, the continuous film production as well as the film materials surface quality. Depending on the size of the dispersed particles the produced films exhibit a noticeable roughness. The present work demonstrates that the preparation of TPS/PBS compounds with a fine dispersion of starch inside

of the polyester matrix is only possible under accelerated shearing conditions, which can be achieved at an increased extrusion screw speed. The synthesis of compatibilizers was conducted on the basis of TPS and native starch. Solubility tests demonstrated that the TPS-based compatibilizer formed a stable suspension in contact with chloroform. In case of the native starch-based compatibilizer only a limited stability was given. Destructurized starch in the form of TPS provided a larger interaction surface (amylose/amylopectin—PBS, and probably also glycerol—PBS) and enabled a better homogenization during the course of compounding. This is why the TPS-based compatibilizer facilitated a significant increase in tensile strength and tear resistance, while the utilization of the starch-based variant only resulted in minor effects. The investigation resulted in a film material with improved mechanical strength, which exhibits a significant potential for single-use, light-weight packaging applications. The applicability of a controlled, separate waste collection for this purpose is doubtful and hence, the compostability under ambient conditions is seen as a benefit. Future investigations will focus on a detailed evaluation and optimization of barrier properties of TPS-based film materials, along with an evaluation of mechanisms that are involved during biodegradation. As the utilization of starch in packaging always induces unwanted opacity instead of full transparency, a potential increase in transparency might be achievable with raw material functionalization, a subject important in follow-up research activities. Furthermore, the effects of varying starch contents and elevated compatibilizer concentrations are subject of ongoing research.

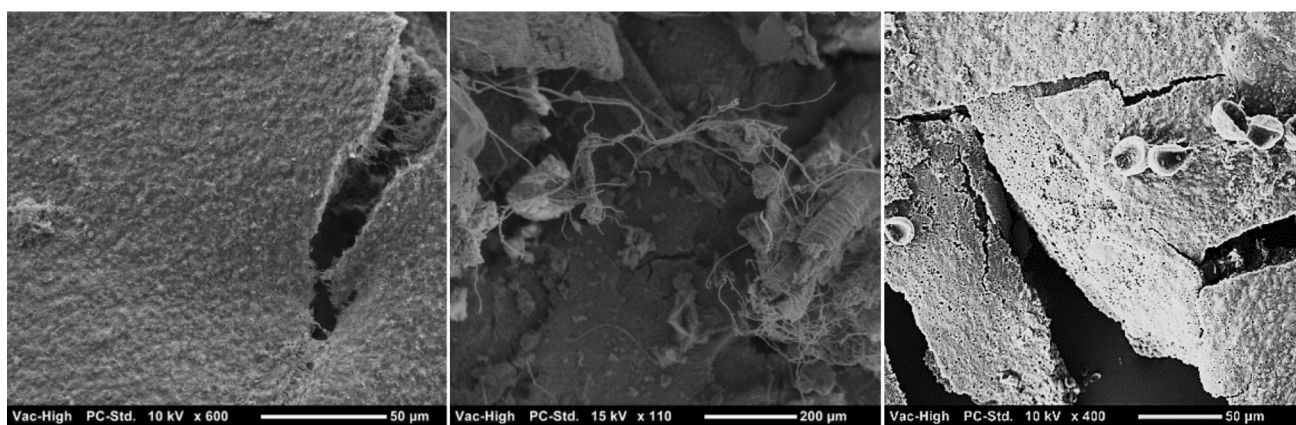


**Fig. 10** Bioplastic-disintegration; formation of cracks (left) and attack by microorganisms (middle, right)

**Acknowledgements** The authors would like to thank the Austrian Research Promotion Agency (FFG, Project Number: 854577) for the financial support. Furthermore, the authors wish to thank Agrana Stärke for generously supplying the required starch raw material.

## References

- Bastioli C (2001) Global status of the production of biobased packaging materials. *Starch* 53:368–371
- Olivato JB et al (2013) Starch/polyester films: simultaneous optimisation of the properties for the production of biodegradable plastic bags. *Polímeros* 23:32–36
- Wang N et al (2007) Influence of citric acid on the properties of glycerol-plasticized dry starch (DTPS) and DTPS/poly(lactic acid) blends. *Starch* 59(9):409–417
- Kalambur S, Rizvi SSH (2006) An overview of starch-based plastic blends from reactive extrusion. *J Plast Film Sheeting* 22(1):39–58
- Ma P et al (2012) Tailoring the morphology and properties of poly(lactic acid)/poly(ethylene)-co-(vinyl acetate)/starch blends via reactive compatibilization. *Polym Int* 61(8):1284–1293
- Wang N, Yu J, Ma X (2007) Preparation and characterization of thermoplastic starch/PLA blends by one-step reactive extrusion. *Polym Int* 56(11):1440–1447
- Maliger RB et al (2006) Compatibilization of starch–polyester blends using reactive extrusion. *Polym Eng Sci* 46(3):248–263
- Al-Itry R, Lamnawar K, Maazouz A (2012) Improvement of thermal stability, rheological and mechanical properties of PLA, PBAT and their blends by reactive extrusion with functionalized epoxy. *Polym Degrad Stab* 97(10):1898–1914
- Mittal V, Akhtar T, Matsko N (2015) Mechanical, thermal, rheological and morphological properties of binary and ternary blends of PLA, TPS and PCL. *Macromol Mater Eng* 300(4):423–435
- Shirai MA et al (2013) Thermoplastic starch/polyester films: effects of extrusion process and poly (lactic acid) addition. *Mater Sci Eng C* 33(7):4112–4117
- Averous L, Dole P, Fringant C (2000) Properties of thermoplastic blends: starch–polycaprolactone. *Polymer* 41:4157–4167
- Liu L et al (2009) Biodegradability of poly(butylene succinate) (PBS) composite reinforced with jute fibre. *Polym Degrad Stab* 94(1):90–94
- Reddy MM et al (2013) Biobased plastics and bionanocomposites: Current status and future opportunities. *Prog Polym Sci* 38(10–11):1653–1689
- Aeschelmann F, Carus M (2017) Biobased building blocks and polymers. Michael Carus (V.i.S.d.P.)
- Zeng JB et al (2011) Bio-based blends of starch and poly(butylene succinate) with improved miscibility, mechanical properties, and reduced water absorption. *Carbohydr Polym* 83:762–768
- Kanitporn SI, Koombhongse P, Chirachanchai S (2014) Starch grafted poly(butylene succinate) via conjugating reaction and its role on enhancing the compatibility. *Carbohydr Polym* 102:95–102
- Li J et al (2013) Comparative study on the blends of PBS/thermoplastic starch prepared from waxy and normal corn starches. *Starch* 65(9–10):831–839
- van den Oever M, Molenveld K (2017) Replacing fossil based plastic performance products by bio-based plastic products—technical feasibility. *New Biotechnol* 37(Pt A):48–59
- Briassoulis D, Giannoulis A (2018) Evaluation of the functionality of bio-based food packaging films. *Polym Testing* 69:39–51
- Siengchin S (2015) Thermomechanical analysis and processing of polymer blends. In: *Characterization of polymer blends: miscibility, morphology and interfaces*. Wiley, Weinheim, pp 393–414
- Fahrngruber B et al (2017) Malic acid: a novel processing aid for thermoplastic starch/poly(butylene adipate-co-terephthalate) compounding and blown film extrusion. *J Appl Polym Sci* 134(48):45539
- Sharma D, MacDonald JC, Iannacchione GS (2006) Thermodynamics of activated phase transitions of 8CB: DSC and MC calorimetry. *J Phys Chem B* 110:16679–16684
- Elabbar AA (2018) Effect of thermal history on crystallization and glass transition in Se and Se90Te10 chalcogenide glasses. *Chalcogenide Lett* 15:515–521
- Zhang Y, Rempel C, Liu Q (2014) Thermoplastic starch processing and characteristics—a review. *Crit Rev Food Sci Nutr* 54(10):1353–1370
- Hancock BC et al (1998) A pragmatic test of a simple calorimetric method for determining the fragility of some amorphous pharmaceutical materials. *Pharm Res* 15(5):762–767
- Seligra PG et al (2016) Biodegradable and non-retrogradable eco-films based on starch-glycerol with citric acid as crosslinking agent. *Carbohydr Polym* 138:66–74
- Cuevas-Carballo ZB, Duarte-Aranda S, Canché-Escamilla G (2017) Properties and biodegradability of thermoplastic starch obtained from granular starches grafted with polycaprolactone. *Int J Polym Sci* 2017:1–13
- Zuo Y et al (2019) Preparation and characterization of hydrophobically grafted starches by in situ solid phase polymerization. *Polymers (Basel)* 11(1):72
- Abu-Bakar AS, Moinuddin KAM (2012) Effects of variation in heating rate, sample mass and nitrogen flow on chemical kinetics for pyrolysis. In: *18th Australasian fluid mechanics conference*, Launceston, Australia
- Khouloud JM, Sabu MC (2017) *Clay-polymer nanocomposites*. Elsevier, Cambridge
- Bouthegeourd E et al (2013) Size of the cooperative rearranging regions vs. fragility in complex glassy systems: influence of the structure and the molecular interactions. *Physica B* 425:83–89
- Tajuddin S et al (2011) Rheological properties of thermoplastic starch studied by multipass rheometer. *Carbohydr Polym* 83(2):914–919
- Ehrenstein GW, Riedel G, Trawiel P (2004) *Thermal analysis of plastics—theory and practice*. Carl Hanser Verlag, München
- Mano JF, Koniarova D, Reos RL (2003) Thermal properties of thermoplastic starch/ synthetic polymer blends with potential biomedical applicability. *J Mater Sci Mater Med* 14:127–135
- Biliaderis CG, Lazaridou A, Arvanitoyannis I (1999) Glass transition and physical properties of polyol-plasticised pullulan–starch blends at low moisture. *Carbohydr Polym* 40:29–47
- Sreenivasan VS et al (2015) Dynamic mechanical and thermogravimetric analysis of *Sansevieria cylindrica*/polyester composite: effect of fiber length, fiber loading and chemical treatment. *Composites B* 69:76–86
- Kulshreshtha AK, Vasile C (2002) *Handbook of polymer blends and composites*, vol 2. Shawbury, Rapra Technology Limited
- Barbosa SE et al (2017) *Starch-based materials in food packaging: processing, characterization and applications*. Elsevier, New York

39. Liu W-C, Halley PJ, Gilbert RG (2010) Mechanism of degradation of starch, a highly branched polymer, during extrusion. *Macromolecules* 43(6):2855–2864
40. Carvalho AJFZ, Curvelo AAS, Gandini A (2003) Size exclusion chromatography characterization of thermoplastic starch composites 1. Influence of plasticizer and fibre content. *Polym Degrad Stab* 79:133–138
41. Willett JL et al (1998) Properties of starch-graft-poly(glycidyl methacrylate)–PHBV composites. *J Appl Polym Sci* 70:1121–1127
42. Mohanty S, Nayak SK (2011) Biodegradable nanocomposites of poly (butylene adipate-co-terephthalate) (PBAT) with organically modified nanoclays. *Int J Plast Technol* 14(2):192–212
43. da Silva NMC et al (2017) PBAT/TPS composite films reinforced with starch nanoparticles produced by ultrasound. *Int J Polym Sci* 2017:1–10
44. Patricia Miranda S et al (2004) Water vapor permeability and mechanical properties of chitosan composite films. *J Chil Chem Soc* 49(2):173–178
45. Dashipour A et al (2014) Physical, antioxidant and antimicrobial characteristics of carboxymethyl cellulose edible film cooperated with clove essential oil. *Zahedan J Res Med Sci* 16(8):34–42

**Publisher's Note** Springer Nature remains neutral with regard to jurisdictional claims in published maps and institutional affiliations.